Laser and Particle Beams (2002), *20*, 93–99. Printed in the USA.

DOI: 10.1017.S0263034602201135

Transverse structures in corona of nonuniformly irradiated solid targets

J. LIMPOUCH,[1] A.B. ISKAKOV,[1,4] K. MAŠEK,[2] K. ROHLENA,[2] I.G. LEBO,[3] AND V.F. TISHKIN[4]

[1]Czech Technical University in Prague, Faculty of Nuclear Sciences and Physical Engineering, Břehová 7, 115 19 Praha 1, Czech Republic
[2]Institute of Physics of the Academy of Sciences of the Czech Republic, Na Slovance 2, 182 21 Praha 8-Libeň, Czech Republic
[3]Lebedev Physical Institute, RAS, Leninskiy pr. 53, 117924 Moscow, Russia
[4]Institute of Mathematical Modeling, RAS, Miusskaya sq. 4a, 125047 Moscow, Russia

(RECEIVED 6 April 2001; ACCEPTED 31 September 2001)

Abstract

Formation of transverse inhomogeneities in the corona of a solid target irradiated by an inhomogeneous main laser pulse and a uniform background pulse was observed experimentally via side-on shadowgraphy. The experimental results were successfully interpreted using a two-dimensional hydrodynamics code. Our simulations identified the onset of sharp contact boundaries between plasma streams of different expansion velocities. The formation and the decay of the contact boundaries is investigated in detail. When the background pulse is used as a laser prepulse, a layer of coronal plasma is formed that enhances main pulse collisional absorption in underdense plasma and creates conditions for an efficient thermal smoothing of the transverse inhomogeneities.

Keywords: Hydrodynamics model; Laser imprint; Laser-produced plasmas; Thermal smoothing

1. INTRODUCTION

The requirement of uniform laser energy deposition on the target is encountered in many direct-drive laser experiments. Various optical smoothing methods have been invented and applied, but these methods are, in principle, unable to eliminate the problem of laser beam nonuniformities on shorter time scales (Desselberger *et al.*, 1992, 1995; Taylor *et al.*, 1996). A promising way how to overcome this difficulty is to employ the thermal conductivity of the plasma as is done by a construction of the complex (sandwich) targets with a buffer foam and a thin metal layer on its top (Dunne *et al.*, 1995). A suitable ablation-critical surface distance is controlled by the thickness of the plastic foam within which the lateral thermal conduction is sufficient to smooth out the nonuniformities imprinted by the laser.

A similar effect is achievable by using a double pulse for directly driven targets. This idea was suggested by Mead and Lindl (1976) and experimentally tested by Mašek *et al.*, (1996). Such a scheme uses a prepulse of a longer wavelength to create an expanding plasma before the arrival of the heating shorter-wavelength laser pulse. A considerable reduction of the inhomogeneities can be achieved when the time delay between the prepulse and the main pulse is optimal (Mašek *et al.*, 1996; Iskakov *et al.*, 2000*b*).

In this contribution, the structures induced by an inhomogeneous target illumination in the expanding corona of solid foil targets are studied. The density structures in the expanding corona are identified by side-on laser shadowgraphy using a diagnostic probe laser beam with variable time delay with respect to the heating laser pulse. A special methodology based on two-dimensional hydrodynamics simulations is introduced for modeling the three-dimensional experimental configuration. The density structures in expanding plasma corona are characterized and their temporal evolution is identified in simulations.

2. EXPERIMENTAL SETUP

The experiments were performed using the iodine photodissociation laser system PERUN (wavelength 1.315 μm, pulse duration 0.5 ns, and output energy 50 J), which was installed at the Institute of Physics of the Academy of Sciences in Prague. For the purpose of this experiment, laser radiation was converted into the third harmonics and the residual infrared part served for the formation of the background pulse. The main and the background pulse were focused

Address correspondence and reprint requests to: J. Limpouch, Faculty of Nuclear, Sciences and Physical Engineering CTU, Břehová 7, 115 19 Praha 1, Czech Republic. E-mail: limpouch@siduri.fjfi.cvut.cz

normally onto a 7-μm-thick Al foil. Nonuniform irradiation conditions on the target were accomplished by splitting the main pulse via inserting an optical wedge in the beam path, forming in this way two focal spots with 80% of the energy confined inside their 20-μm radius. The distance between the spot centers was 80 μm, and main pulse energy impinging inside each spot was 1.25 J. These spots are placed inside a large circular focus with 100-μm radius of the infrared background beam of 10 J energy. The focal geometry is shown in Figure 1a. The temporal shape of both the laser pulses was close to a Gaussian form with a pulse duration of 500 ps FWHM. The time delay of the main pulse with respect to the background pulse was varied in the range from 0 to 1.5 ns. Two pinhole cameras with ~10-μm spatial resolution were used to investigate plasma nonuniformity; the first one was located in a side-on position with respect to the target, and the other one viewed the rear side. The second method used to study the hydrodynamics of the thin Al-foil target under the double pulse irradiation was an optical shadowgraphy technique. The optical probe beam of frequency 3ω was derived by splitting a fraction of the main beam in order to ensure synchronization. The shadowgraphs were recorded by a CCD camera. Unfortunately, the port configuration of the target chamber did not allow for a simultaneous recording of both the X-ray images and of the optical shadowgraph.

3. SIMULATION

The plasma evolution is simulated by a cylindrical version of two-dimensional Lagrangian code "ATLANT-C" (Lebo *et al.*, 1996; Iskakov *et al.*, 1997), based on a one-fluid two-temperature hydrodynamics model. The value $f = 0.05$ is used for the flux limiter inhibiting the classical heat conductivity. The mean ion charge is calculated in a nonstationary average atom approximation. Propagation of laser beams in the underdense plasma is modeled in the approximation of geometrical optics via a ray-tracing algorithm (Iskakov *et al.*, 2000*a*). Collisional absorption of the laser radiation in the underdense plasma is included. As the spatial resolution of the hydrocode is not sufficient for an exact calculation of laser absorption, we assumed full absorption of the laser radiation entering the cell of the hydrocode, where the ray is reflected. To account for the estimated experimental absorption efficiency (Eidmann *et al.*, 1984), the incident background pulse intensity is multiplied by a factor of 0.4, while the intensity of the main blue pulse is multiplied by a factor of 0.7.

In the simulations, the main pulse is assumed to have an annular ring shape (see Fig. 1b), as the model does not allow for the true experimental geometry, which is intrinsically three-dimensional. It is expected that this geometry will preserve the basic features of the coronal plasma expansion. The diameter of this ring is taken to be equal to the experimental distance of 80 μm between the main pulse focal spot centers. The peak laser intensity within the ring $I_m = 2.4 \times 10^{14}$ W/cm^2 is equal to the experimental main pulse intensity in the spot centers. Main pulse energy is derived from the requirement that laser energy per area inside the ring in simulations would be equal to the experimental energy in laser spots per area between them. The width of the annular ring is derived from the laser energy and intensity. Gaussian spatial distribution is assumed with 80% of laser energy

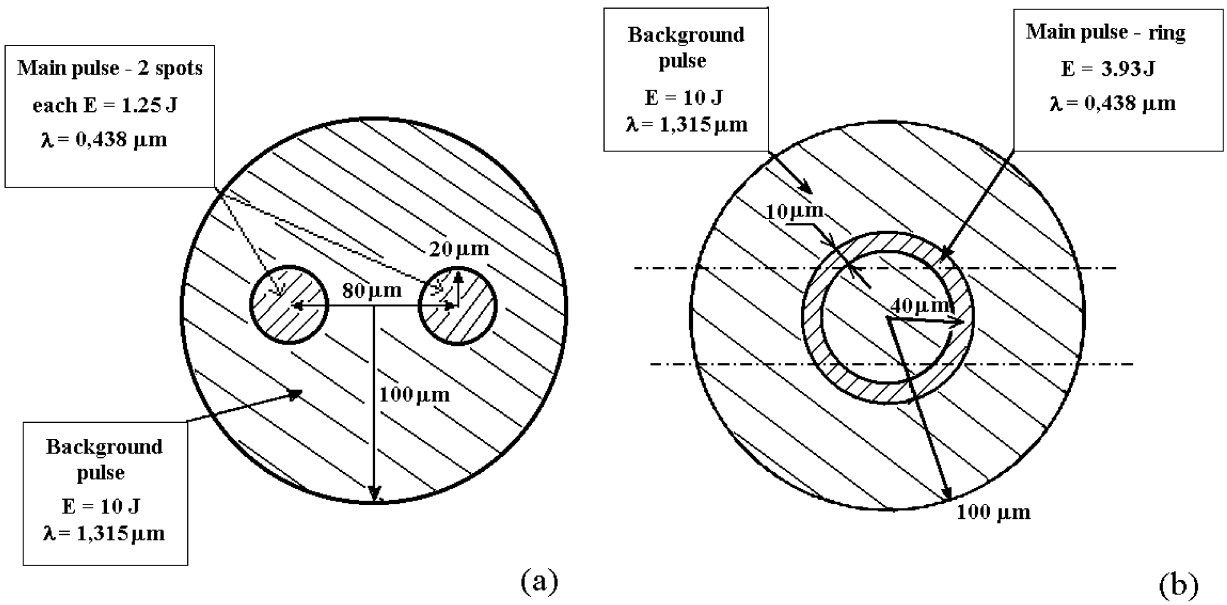

Fig. 1. Target illumination scheme (focal plane) in the experiment (a) and in the simulation (b). The slab used for the shadowgraph reconstruction is denoted by the dashed horizontal lines.

https://doi.org/10.1017/S0263034602201135 Published online by Cambridge University Press

inside the 10-μm width of the annular ring. The geometry used here is different from our previous simulations (Iskakov *et al.*, 2000*b*) of the foil acceleration, where only a single spot was considered.

To have a possibility of a direct comparison of simulations with the experiment, the results of hydrodynamics simulations are postprocessed and synthetic shadowgraphs are calculated. Here, a 50-μm-thick plasma slab is assumed with plasma parameters taken from hydrodynamics simulations in the plane including the symmetry axis of the cylindrical geometry. The algorithm used for the ray tracing of the probe beam takes into account both the refraction and the absorption inside the slab. The bounds given by the angular aperture of the imaging lens with focal length f = 6 cm and the sensitive area of the CCD element are taken into account. The calculated shadowgraphs are temporally integrated over the probe beam pulse.

4. COMPARISON OF SYNTHETIC AND EXPERIMENTAL SHADOWGRAPHS

The experimental and the synthetic shadowgraphs are displayed in Figure 2 for the main pulse delay $\Delta\tau = 0.5$ ns (left) and for the simultaneous incidence of the background and the main pulse $\Delta\tau = 0$ (right). Here, the delay of the probing beam with respect to the main pulse is 0.3 ns in all cases. Despite the intrinsic limitation of the hydrodynamic simulations to a 2D cylindrical geometry, the experimental side-on view shadowgraphs are successfully reproduced. A qualitative agreement between the experiment and the simulation in the expansion of the front and rear side of the foil target is apparent. Both the experimental and synthetic shadowgraphs show a significant smoothing of the transverse structures in plasma corona when the laser prepulse is applied by 0.5 ns ahead of the main pulse.

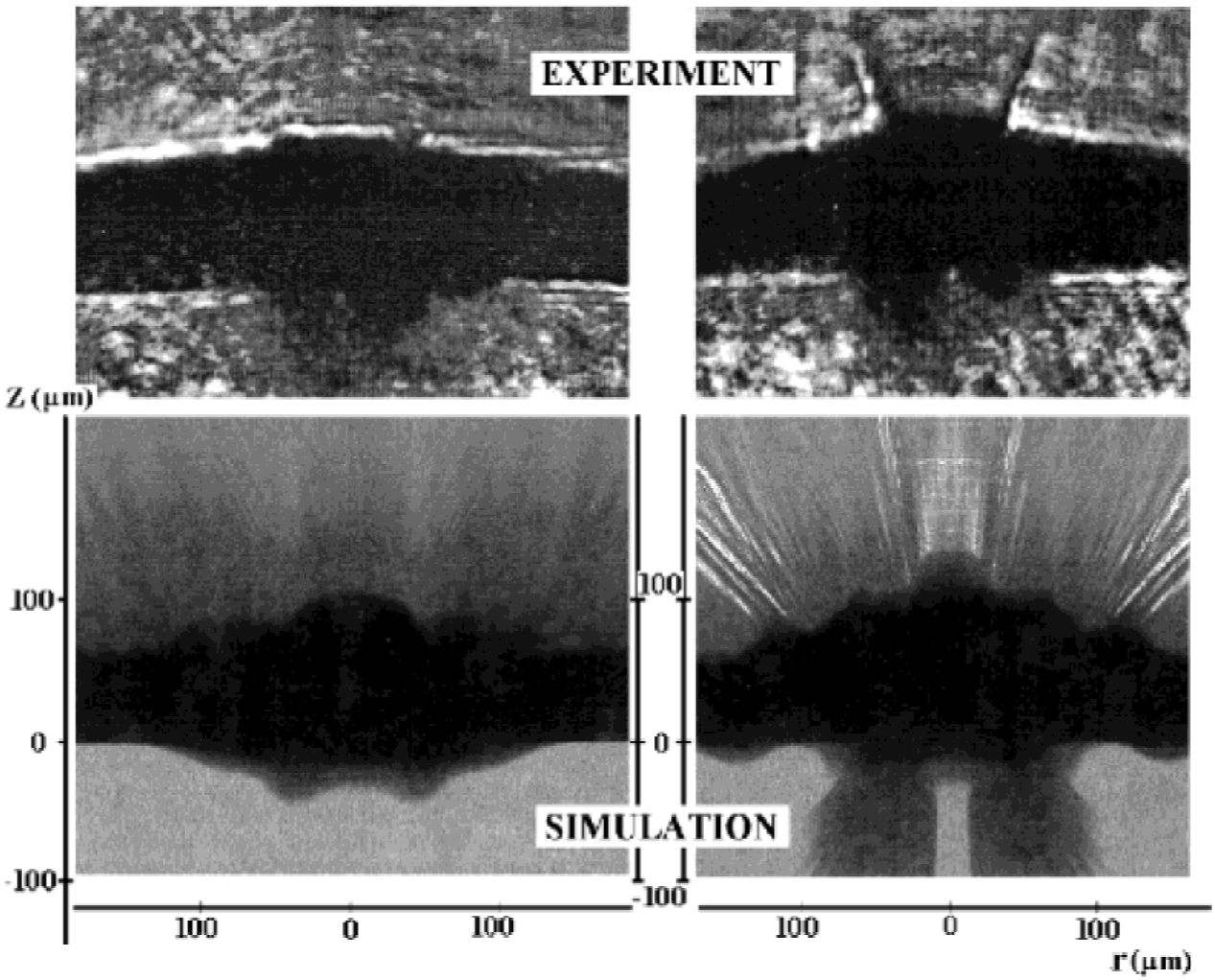

Fig. 2. The experimental and synthetic side-on view shadowgraphs taken with the probe beam delayed by 0.3 ns with respect to the main pulse. The delay of the main pulse with respect to the background pulse is 0.5 ns (left) and 0 ns (right). The laser beams are incident from the top along the z-axis, the initial foil position z = 0–7 μm, focal plane center r = 0.

https://doi.org/10.1017/S0263034602201135 Published online by Cambridge University Press

Both the experiments and the simulations show a dark layer near the target surface inaccessible for the shadowgraphy. A good agreement between simulations and experiment in the form and the size of this area is demonstrated. The form of the dark area boundary at the rear side of the foil shows a diminishing inhomogeneity of the foil acceleration for the delay $\Delta\tau = 0.5$ ns; however, some inhomogeneity is still visible. A similar conclusion can be derived from the rear-side pinhole camera images.

Intense jetting outside the focal spot region on the irradiated side occurs if the aluminum target is driven by a double pulse with zero time delay. No smoothing effect is observed in this case. When the background pulse is used as a prepulse by 0.5 ns and longer ahead of the main pulse, the jetting appears to be much less pronounced and the formation of the contact boundaries is suppressed.

5. INTERPRETATION OF THE TRANSVERSE STRUCTURES

The dynamics of the formation of transverse structures in the expanding corona is revealed when the density contours are plotted in a sequence of points in time. When the contours are plotted in *r*–*z* coordinates, the symmetrical reflection of the picture with respect to the *z* axis is added to imitate the geometry of side-on view shadowgraphs.

A sequence of density contour plots calculated for the case of simultaneously incident background and main pulse ($\Delta\tau = 0$) is displayed in Figure 3. Plasma streams with different ablation characteristics are formed here, as the absorbed intensity within the ring and in its center differs for 7 times (1.7×10^{14} W/cm^2 and 2.5×10^{13} W/cm^2, respectively). These plasma streams are colliding laterally and distinct contact boundaries are formed with substantial discontinuities in plasma density and in tangential velocity (shear). The simulation shows that the contact boundaries in the expanding plasma develop at approximately 0.2 ns ahead of the laser pulse maximum. They persist for an interval of 0.3 ns as spatially stable and static structures. The observed structures cannot be interpreted as filaments induced by laser ponderomotive or thermal filamentation (Limpouch & Rozanov, 1984) as their direction differs from the incident laser beam.

The geometry of the experiment leads to a confinement of the low ablation area between two areas with an intense ablation. Thus the position of contact boundaries is fixed for the above interval and the boundaries can be easily registered by means of laser shadowgraphy. The lifetime of the observed contact boundaries is determined by the thermal smoothing in the corona. The predominant factor of the formation of contact boundaries is the inhomogeneity of laser irradiation. When a substantial plasma layer is formed, thermal conduction starts to smooth the inhomogeneities in plasma temperature. Later, the hydrodynamic flow smooths the density profile and the contact boundaries are washed out. The scheme of the contact boundaries formation and decline is demonstrated in Figure 4. Our simulations indicate that stable spatial structure of a particular shape may be formed by using an appropriate geometry of target irradiation. In principle, such structures might be potentially important for some applications such as X-ray laser media and plasma waveguides (Rus *et al.*, 1997).

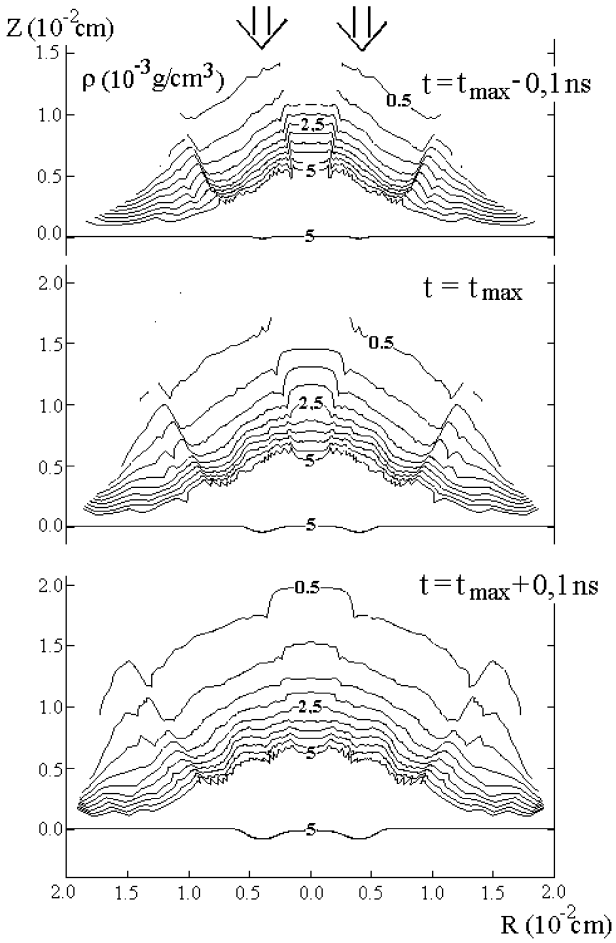

Fig. 3. Density contours plotted at different time points (laser pulse maximum at t_{max}), when the main and the background pulse are incident at the same time ($\Delta\tau = 0$). Symmetrical pictures with the respect to the *z* axis are plotted in order to imitate the geometry of side-on view shadowgraphs.

Our simulations show that the absence of the background laser pulse changes the mode of plasma expansion considerably. The sequence of density contour plots, displayed in Figure 5, demonstrates the formation of a narrow cumulative jet in the ring center due to collision of expanding plasma streams. Thus, the background pulse is crucial for the formation of the contact boundaries.

6. PREPULSE-INDUCED THERMAL SMOOTHING

When the main pulse is incident with delay $\Delta\tau = 0.5$ ns after the background prepulse, contact boundaries are observed neither in the shadowgraphs (Fig. 2) nor in Figure 6, where

https://doi.org/10.1017/S0263034602201135 Published online by Cambridge University Press

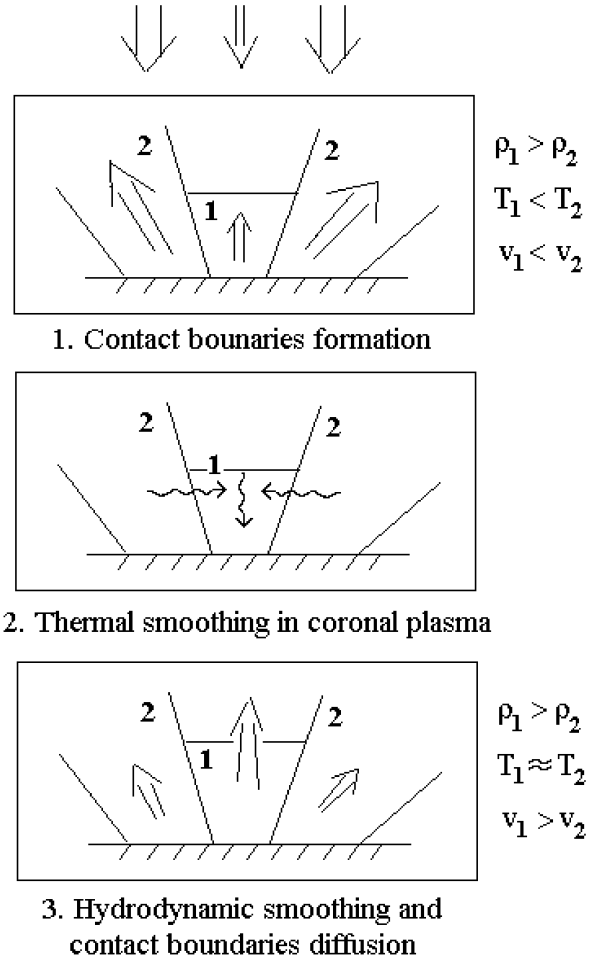

Fig. 4. Scheme of contact boundaries formation and decay.

the calculated density contours are plotted. Uniform background pulse creates a layer of the hot coronal plasma, where the transverse inhomogeneities are effectively smoothed out by the lateral thermal transport.

The mechanism of the smoothing by laser prepulse can be elucidated by comparing the spatial distributions of the absorbed laser power densities, displayed in Figure 7 at the time point 0.1 ns before the main pulse maximum. The plasma formed by the prepulse enhances collisional absorption of the main laser beam during its propagation towards the critical surface. A nonnegligible part of the laser energy is absorbed far from the critical surface, and consequently, lateral thermal transport in the underdense plasma adds considerably to the thermal smoothing.

Moreover, the power absorbed in the vicinity of the critical surface is approximately 1.5–2 times lower than in the case of the simultaneously incident background and the main pulse. As a consequence, the mass ablation rate is also roughly 1.5–2 times lower and it is significantly smoothed both in time and along the radius. The impact of the main pulse delay on the mass ablation rate is demonstrated in Figure 8, where mass ablation rate is plotted versus radius and time.

Finally, plasma expansion velocities are lower for the main pulse delay $\Delta\tau = 0.5$ ns, and, thus, a longer time interval is available for the smoothing of the nonuniformities by thermal and hydrodynamics processes in the expanding plasma. For both cases, the longitudinal (normal to the foil surface) velocities of the expanding plasmas are plotted in Figure 9 in the moment of the main pulse maximum.

7. CONCLUSIONS

The formation of transverse inhomogeneities in the plasma corona was studied both experimentally and via hydrodynamics simulations using a special form of target irradiation. Experimental side-on view shadowgraphs are successfully reproduced by the hydrodynamic simulations, despite their intrinsic limitation to the 2D cylindrical geometry.

The simulations indicate that the most pronounced transverse structures may be interpreted as contact boundaries between adjacent plasma areas characterized by different plasma densities and expansion velocities, induced by the nonuniformities in the target illumination. Stable contact

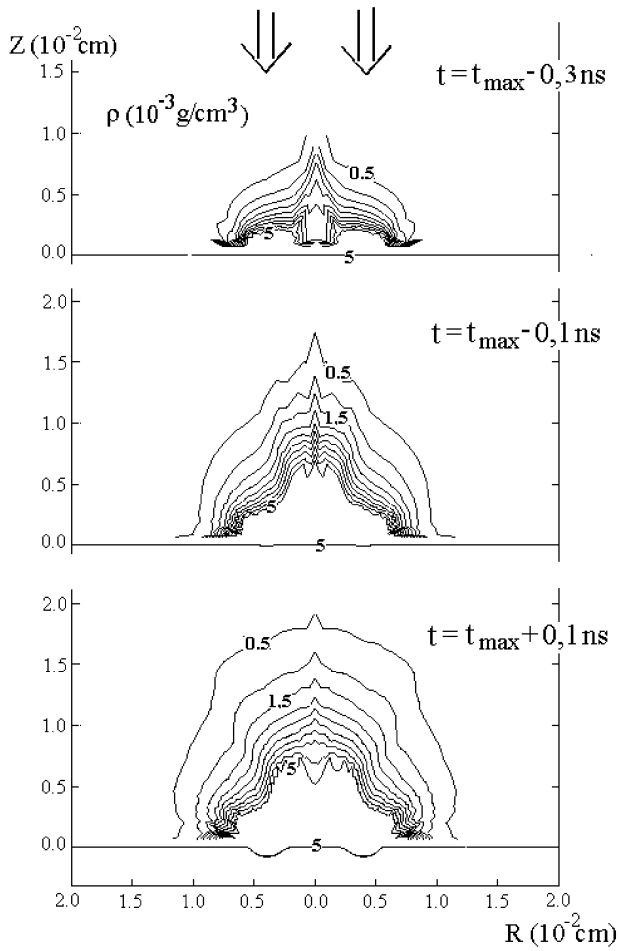

Fig. 5. Sequence of plasma density profiles calculated for the case when the background pulse is absent.

https://doi.org/10.1017/S0263034602201135 Published online by Cambridge University Press

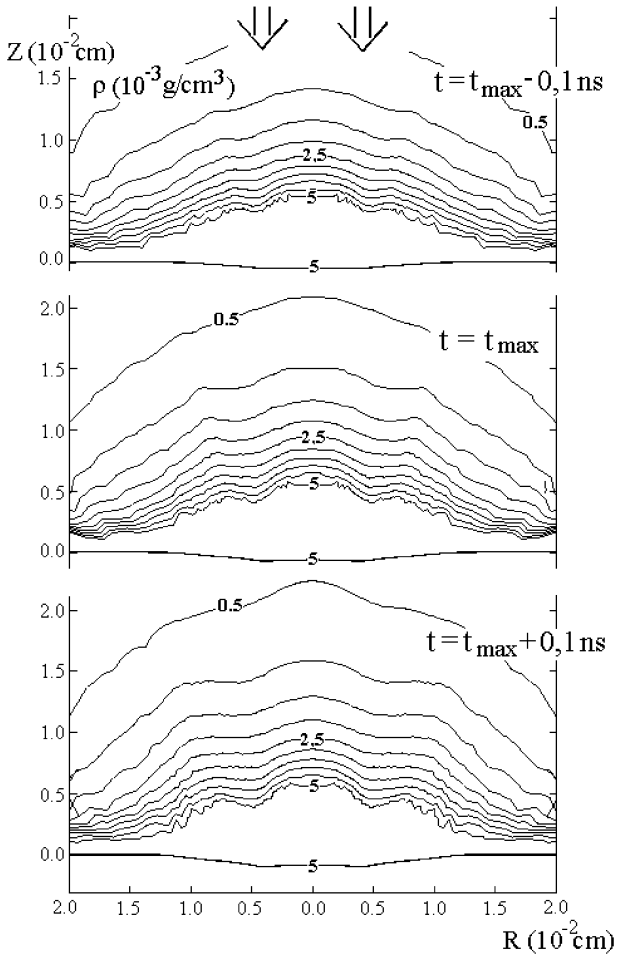

Fig. 6. Sequence of plasma density profiles (main pulse maximum at t_{max}) calculated for the case when the main pulse is delayed by $\Delta\tau = 0.5$ ns with respect to the background pulse.

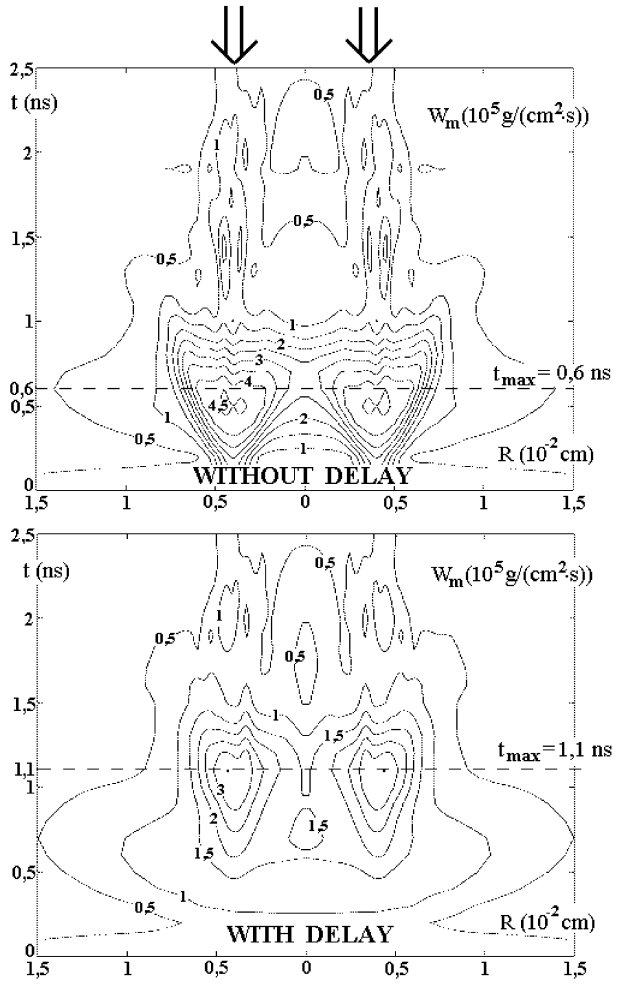

Fig. 8. Mass ablation rates ($r - t$ profiles) for the main pulse delay $\Delta\tau =$ 0 ns (top) and $\Delta\tau = 0.5$ ns (bottom).

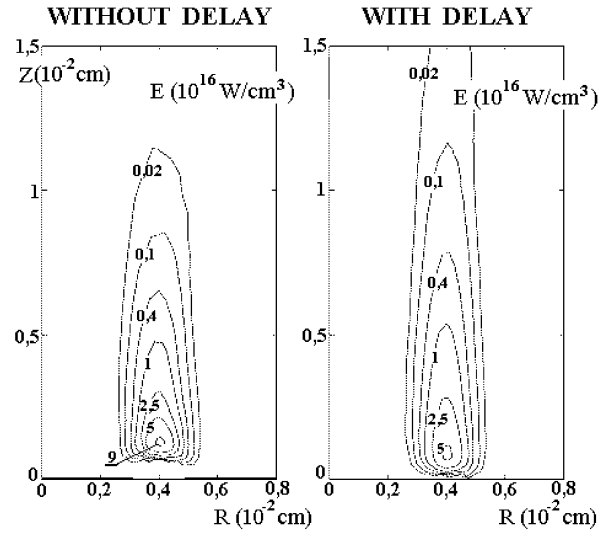

Fig. 7. Spatial distribution of absorbed power densities plotted at the time point 0.1 ns before the main pulse maximum. The main pulse delay is $\Delta\tau =$ 0 ns (left) and $\Delta\tau = 0.5$ ns (right).

boundaries are observed in our simulations for a relatively long period of time near the main pulse maximum. During this interval their position and angle to the target surface remain unchanged. Thus, our simulations indicate that a special geometry of target irradiation can be applied to create stable density structures in expanding plasmas that might be potentially important for applications.

A laser prepulse of lower intensity can induce considerable smoothing of the transverse inhomogeneities in the expanding plasma corona when it is applied at a suitable time prior to the arrival of the main pulse. The smoothing of transverse structures in the expanding plasma may be beneficial for applications where forming of a homogeneous plasma layer is required. The physics of the smoothing is based on enhanced collisional absorption in underdense plasma. Intensity absorbed in the vicinity of the critical surface drops. Consequently, the mass ablation rate is decreased and smoothed in time and along the radius. Direct-drive laser fusion may profit from the reduction of laser nonuniformity imprint on the ablation surface.

https://doi.org/10.1017/S0263034602201135 Published online by Cambridge University Press

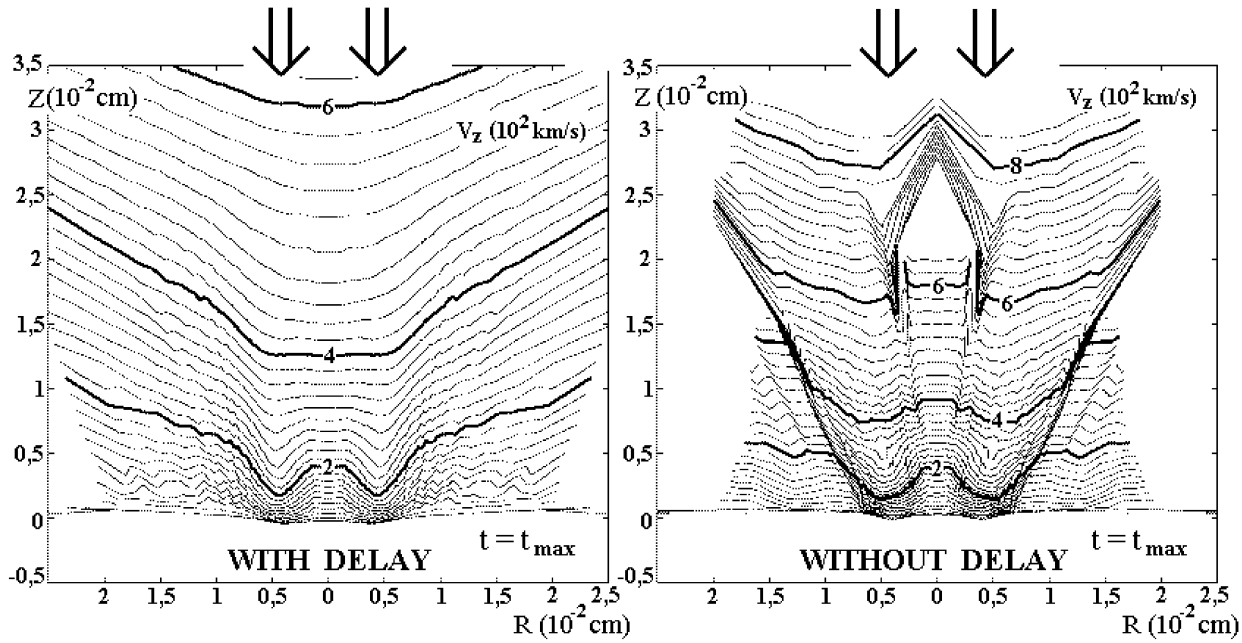

Fig. 9. Spatial profiles of longitudinal (normal to the target surface) velocities plotted at the main pulse maximum. The main pulse delay is $\Delta\tau = 0.5$ ns (left) and $\Delta\tau = 0$ ns (right).

ACKNOWLEDGMENTS

The support of J.L., A.B.I., K.M., and K.R. by the Ministry of Education of the Czech Republic in the frame of the project Laser Plasma Research Centre (LN00A100) is gratefully acknowledged. The work of I.G.L and V.F.T. was partially supported by the grant N00-02-17188 of the Russian Foundation of Fundamental Research.

REFERENCES

Desselberger, M., Afsharrad, T., Khattak, F., Viana, S. & Willi, O. (1992). Nonuniformity imprint on the ablation surface of laser-irradiated targets. *Phys. Rev. Lett.* **68**, 1539–1542.

Desselberger, M., Jones, M.W., Edwards, J., Dunne, M. & Willi, O. (1995). Use of X-ray preheated foam layers to reduce beam structure imprint in laser-driven targets. *Phys. Rev. Lett.* **74**, 2961–2964.

Dunne, M., Borghesi, M., Iwase, A., Jones, M.W., Taylor, R., Willi, O., Gibson, R., Goldman, S.R., Mack, J. & Watt, R.G. (1995). Evaluation of a foam buffer target design for spatially uniform ablation of laser-irradiated plasmas. *Phys. Rev. Lett.* **75**, 3858–3861.

Eidmann, K. Amiranoff, F., Fedosejevs, R., Maaswinkel, A.G.M., Petch, R., Sigel, R., Spindler, G., Teng, Y., Tsarikis, G. & Witkowski, S. (1984). Interaction of 1.3-μm laser-radiation with thin foil targets. *Phys. Rev. A* **30**, 2568–2589.

Iskakov, A.B., Lebo, I.G., Popov, I.V, Rozanov, V.B. & Tishkin, V.F. (1997). On the inclusion of laser ray refraction in the simulation of 20-nonuniform target compression. *Kratkie soobscheniya po fizike*, No. 1-2, 28–36. [*Bulletin of the Lebedev Physics Institute*, No. 1, 23–30].

Iskakov, A.B, Lebo, I.G. & Tishkin, V.F. (2000*a*). 2D numerical simulation of the interaction of high-power laser pulses with plane targets using the "ATLANT-C" Lagrangian code. *J. Russian Laser Res.* **21**, 247–263.

Iskakov, A.B., Tishkin, V.F., Lebo, I.G., Limpouch, J., Mašek, K. & Rohlena, K. (2000*b*). Two-dimensional model of thermal smoothing of laser imprint in a double-pulse plasma. *Phys. Rev. E* **61**, 842–847.

Lebo, I.G., Rohlena, K., Rozanov, V.B. & Tishkin, V.F. (1996). Symmetrising influence of a laser prepulse on the development of perturbations of the shell-fuel contact boundary. *Kvantovaya Elektronika* **23**, 71–72. [*Sov. J. Quantum Electronics* **26**, 69–70].

Limpouch, J. & Rozanov, V.B. (1984). Transverse structures (filaments, spicules, jets) in laser plasma. *Kvantovaya Elektronika* **11**, 1416–1424 [*Sov. J. Quantum Electronics* **14**, 955].

Mašek, K., Králiková, B., Láska, L., Přeučil, S., Rohlena, K., Skála, J., Straka, P., Bessarab, A.V., Garanin, S.G., Kiryanov, Yu.F., Kochemasov, G.G., Lvov, L.V., Ryadov, A.B., Sukharev, S.A., Suslov, N.A., Vinokurov, O.A. & Zaretskiy, A.I. (1996). Self-smoothing effect of double-pulse-laser plasma. *Proc. SPIE* **2767**, 90–95.

Mead, W.C. & Lindl, J.D. (1976). Symmetry and illumination uniformity requirements for high density laser-driven implosions. *Bull. Am. Phys. Soc.* **21**, 1102.

Rus, B., Zeitoun, P., Mocek, T., Sebban, S., Kálal, M., Demir, A., Jamelot, G., Klisnick, A., Králiková, B., Skála, J. & Tallents, G.J. (1997). Investigation of Zn and Cu prepulse plasmas relevant to collisional excitation X-ray lasers. *Phys. Rev. A* **56**, 4229–4241.

Taylor, R.J., Dahlburg, J.P., Iwase, A., Gardner, J.H., Fyfe, D.E. & Willi, O. (1996). Measurement and simulation of laser imprinting and consequent Rayleigh–Taylor growth. *Phys. Rev. Lett.* **76**, 1643–1646.

https://doi.org/10.1017/S0263034602201135 Published online by Cambridge University Press